Proceedings of the 11th Brazilian Congress of Thermal Sciences and Engineering -- ENCIT 2006
Braz. Soc. of Mechanical Sciences and Engineering -- ABCM, Curitiba, Brazil, Dec. 5-8, 2006

Paper CIT06-0654

ANALYSIS OF HYPERBOLIC HEAT CONDUCTION IN FINS THROUGH THE GENERALIZED INTEGRAL TRANSFORM TECHNIQUE

Carlos Alexandre Moreira da Silva
Emanuel Negrão Macêdo
João Nazareno Nonato Quaresma
Chemical and Food Engineering Department, CT, Universidade Federal do Pará, UFPA
Campus Universitário do Guamá, 66075-110, Belém, PA, Brazil; quaresma@ufpa.br

Renato Machado Cotta
Mechanical Engineering Department – POLI/COPPE, Universidade Federal do Rio de Janeiro, UFRJ
Cx. Postal 68503 – Cidade Universitária, 21945-970, Rio de Janeiro, RJ, Brazil; cotta@serv.com.ufrj.br

Abstract. *The Generalized Integral Transform Technique (GITT) is employed in the hybrid solution of the energy equation to describe the behavior of a rectangular fin undergoing non-Fourier heat conduction. The employment of the GITT approach in the hyperbolic heat conduction equation leads to a coupled system of second order ordinary differential equations in time. The resulting system is then numerically solved by Gear`s method for stiff problems, available in the subroutine DIVPAG from the IMSL Library. Numerical results for the temperature field are computed for different values of the governing parameters and dimensionless thermal relaxation times, which are then compared with results previously reported in the literature for special cases.*

Keywords. *Hyperbolic heat conduction, Rectangular fins, Integral transforms, Hybrid methods.*

1. Introduction

Non-Fourier hyperbolic models have been proposed to investigate conduction heat transfer phenomenon in a few special applications, such as in some situations related to combustion engines, pulsating laser heating, rapidly contacting surfaces in electronic devices and heat transfer in nanosystems. For these situations, the classical model based on the Fourier law is not adequate to describe the physical mechanism of heat conduction, in which the speed of propagation of thermal waves is infinite, this way leading to a non-realistic notion of energy diffusion. The technological advances in the micro- and nano-fabrication fields, including the construction of micro heat exchange devices, has contributed to the appearance of investigations towards the evaluation of performance and efficiency of fins, when heat propagates in extremely short time intervals with a finite speed of propagation. In order to take into account the effect of finite speed thermal transfers, Cattaneo (1958) and Vernotte (1958) independently modified the Fourier model to include a relaxation time that reflects the temporary delay of the thermal wave. In their models, the Fourier law is a particular case when the relaxation time is zero, and thus an infinite speed of thermal wave propagation is achieved, as foreseen by this classical theory.

Many researchers have devoted attention to heat transfer in fast processes along the years. More recently, Tsai et al. (2005) analyzed the non-Fourier effect on the thermal behavior of spherical media (hollow and bi-layered composite spheres) subjected to suddenly changes of the surface temperature. These authors focused their analysis in using the Laplace transform in conjunction with the Riemann-sum approximation method to solve the related energy equation and to investigate the influence of parameters such as relaxation time, temperature and diffusivities ratio. Quaresma et al. (2001), Cruz et al. (2001) and Macêdo et al. (2005) solved the hyperbolic heat conduction problem for a slab subjected to various prescribed heat flux forms at one of the boundaries. Different methodologies were employed to solve the hyperbolic heat conduction equation, respectively, Laplace Transforms with numerical inversion (Quaresma et al., 2001), Finite Volume Method with Gear Approach (Cruz et al., 2001) and the Generalized Integral Transform Technique (Macêdo et al., 2005). Numerical results for the temperature field were presented in order to analyze the influence of the governing parameters (relaxation times and Biot numbers) on this physical problem. In dealing with heat flow in fins, Lin (1998) studied the effect of the relaxation time on the performance of a convective fin of constant cross-sectional area subjected to periodic thermal conditions, by employing a hybrid scheme involving the Laplace transform and the finite volume method.

In this context, the main objective of the present work is to develop a hybrid numerical-analytical solution based on the Generalized Integral Transform Technique (GITT) (Cotta, 1993; Cotta, 1994; Cotta& Mikhailov, 1997; Cotta & Mikhailov, 2006) to analyze the non-Fourier thermal response of a fin of constant cross-sectional area, such as the one studied by Lin (1998). The employment of the GITT approach to solve the related hyperbolic partial differential equation produces a fast and efficient solution, with a considerable analytical involvement, but presenting some advantages when compared to purely numerical schemes. The characteristic of automatic global error control inherent to this technique allows for the computation of benchmark results as well. In this case, the integral transformation of the hyperbolic partial differential equation yields an infinite system of coupled ordinary differential equations of second order, which is then solved through well-established routines appropriate for handling initial value problems with stiff characteristics, such as the DIVPAG routine from the IMSL Library (1991). Numerical results are then produced for the temperature field within representative ranges of the governing parameters, and critically compared with those previously presented in the literature.

2. Analysis

One-dimensional hyperbolic heat conduction in a fin of constant cross-sectional area is considered, initially at the uniform temperature T_i, assuming constant thermophysical properties k and α, and no internal heat generation. The fin tip is maintained insulated, while its larger surfaces are exchanging heat by convection with a fluid kept at a constant temperature, T_∞ and uniform heat transfer coefficient, h. The fin base is subjected to a periodic temperature variation in the form:

$$T_b(t) = \overline{T}_b + (\overline{T}_b - T_i)A\cos(\hat{\omega}t)\,,\ t > 0 \tag{1}$$

where $\overline{T}_b$ is the average fin base temperature, A is the dimensionless amplitude of base temperature difference oscillation and $\hat{\omega}$ is the frequency of base temperature oscillation. The heat transfer by radiation is neglected and the heat transfer coefficient, h, is varying with the spatial coordinate as:

$$h(x) = h_0 H(x/L) \tag{2}$$

where h_0 is a reference heat transfer coefficient, which is taken as $h_0 = bk/(2L^2)$ and H is a function only of the spatial coordinate.

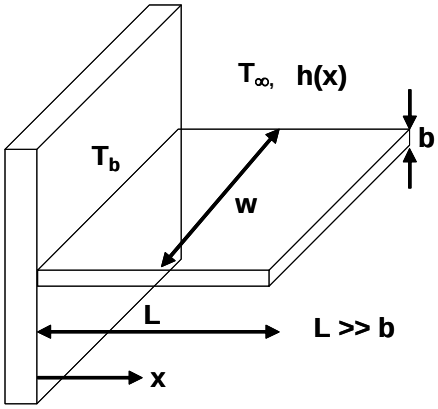

Figure 1. Schematic representation of the fin geometry.

The one-dimensional energy equation for the fin shown in Fig. (1) is written in the following form:

$$\rho c_p \frac{\partial T(x,t)}{\partial t} = -\frac{\partial q''(x,t)}{\partial x} - 2\frac{h(x)}{b}[T(x,t) - T_\infty] \tag{3}$$

For the phenomenon involving finite speed of propagation of the thermal waves, the classical Fourier model must be modified. Therefore, Cattaneo (1958) and Vernotte (1958) independently derived a model of heat flow in the form:

$$\tau_r \frac{\partial q''(x,t)}{\partial t} + q''(x,t) = -k\frac{\partial T(x,t)}{\partial x} \tag{4}$$

where τ_r is the relaxation time of the material in which the heat conduction process is occurring. Combining Eq. (3) with Eq. (4), it then results the partial differential equation that governs the hyperbolic heat conduction in a convective fin, as:

$$\rho c_p \tau_r \frac{\partial^2 T(x,t)}{\partial t^2} + \rho c_p \frac{\partial T(x,t)}{\partial t} + 2\tau_r \frac{h(x)}{b}\frac{\partial [T(x,t) - T_\infty]}{\partial t} = k\frac{\partial^2 T(x,t)}{\partial x^2} - 2\frac{h(x)}{b}[T(x,t) - T_\infty] \tag{5}$$

Equation (5) describes the heat propagation in a convective fin with speed $\nu = (\alpha/\tau_r)^{1/2}$. Equation (5) is then written in dimensionless form as:

$$\beta\frac{\partial^2\theta(\eta,\xi)}{\partial\xi^2} + [1+\beta H(\eta)]\frac{\partial\theta(\eta,\xi)}{\partial\xi} = \frac{\partial^2\theta(\eta,\xi)}{\partial\eta^2} - H(\eta)\theta(\eta,\xi) + H(\eta)\theta_e \tag{6a}$$

subjected to the following initial and boundary conditions:

$$\theta(\eta,0) = 0\,;\quad \frac{\partial\theta(\eta,0)}{\partial\xi} = 0,\quad 0 \le \eta \le 1 \tag{6b,c}$$

$$\theta(0,\xi) = 1 + A\cos(\omega\xi)\,;\quad \frac{\partial\theta(1,\xi)}{\partial\eta} = 0,\quad \xi > 0 \tag{6d,e}$$

The following dimensionless groups were employed in obtaining Eqs. (6):

$$\eta = x/L; \quad \xi = \alpha t/L^2; \quad \beta = \alpha\tau_r/L^2; \quad \omega = \hat{\omega}L^2/\alpha; \quad \theta(\eta,\xi) = [T(x,t) - T_i]/[\overline{T}_b - T_i]; \quad \theta_e = [T_\infty - T_i]/[\overline{T}_b - T_i] \tag{7}$$

Equations (6) constitute a non-homogeneous problem, which have to be filtered in order to obtain a better computational performance in the integral transform method. For this purpose, the dimensionless temperature $\theta(\eta,\xi)$ is written in a separated form as follows:

$$\theta(\eta,\xi) = \theta_f(\eta;\xi) + \theta_h(\eta,\xi) \tag{8}$$

Introducing Eq. (8) into Eqs. (6), one obtains the following equations for calculating the filtered potential $\theta_f(\eta,\xi)$:

$$\frac{\partial^2\theta_f(\eta;\xi)}{\partial\eta^2} + H(\eta)\theta_e = 0 \tag{9a}$$

$$\theta_f(0;\xi) = 1 + A\cos(\omega\xi), \quad \xi > 0 \tag{9b}$$

$$\frac{\partial\theta_f(1;\xi)}{\partial\eta} = 0, \quad \xi > 0 \tag{9c}$$

Equation (9a) is readily integrated to yield

$$\theta_f(\eta;\xi) = 1 + A\cos(\omega\xi) + \theta_e\int_0^\eta\int_{\eta'}^1 H(\eta'')d\eta''d\eta' \tag{9d}$$

For the particular case where $H(\eta) = e^\eta$ (the functional form adopted in the illustration of results), Eq. (9d) becomes

$$\theta_f(\eta;\xi) = 1 + A\cos(\omega\xi) + \theta_e(1 + e\eta - e^\eta) \tag{9e}$$

Then, the partial differential equation for the filtered potential $\theta_h(\eta,\xi)$ is obtained as

$$\beta\frac{\partial^2\theta_h(\eta,\xi)}{\partial\xi^2} + [1+\beta H(\eta)]\frac{\partial\theta_h(\eta,\xi)}{\partial\xi} = \frac{\partial^2\theta_h(\eta,\xi)}{\partial\eta^2} - H(\eta)\theta_h(\eta,\xi) - \left[\beta\frac{\partial^2\theta_f(\eta;\xi)}{\partial\xi^2} + [1+\beta H(\eta)]\frac{\partial\theta_f(\eta;\xi)}{\partial\xi} + H(\eta)\theta_f(\eta;\xi)\right] \tag{10a}$$

$$\theta_h(\eta,0) = -\theta_f(\eta;0) = -[1 + A + \theta_e(1 + e\eta - e^\eta)], \quad 0 \le \eta \le 1 \tag{10b}$$

$$\frac{\partial\theta_h(\eta,0)}{\partial\xi} = -\frac{\partial\theta_f(\eta;0)}{\partial\xi} = 0, \quad 0 \le \eta \le 1 \tag{10c}$$

$$\theta_h(0,\xi) = 0, \quad \xi > 0 \tag{10d}$$

$$\frac{\partial\theta_h(1,\xi)}{\partial\eta} = 0, \quad \xi > 0 \tag{10e}$$

2.1. Solution methodology

The next step is to find a solution for the potential $\theta_h(\eta,\xi)$, and for this purpose we follow the ideas in the GITT (Cotta, 1993; Cotta, 1994; Cotta & Mikhailov, 1997; Cotta & Mikhailov, 2006), first by selecting an appropriate auxiliary eigenvalue problem, which shall provide the basis for the eigenfunction expansion. Therefore, the following simple eigenvalue problem is here proposed:

$$\frac{d^2\psi_i(\eta)}{d\eta^2} + \mu_i^2\psi_i(\eta) = 0, \quad \text{in} \quad 0 < \eta < 1 \tag{11a}$$

$$\psi_i(0) = 0; \quad \frac{d\psi_i(1)}{d\eta} = 0 \tag{11b,c}$$

Equations (11) can be analytically solved to yield, respectively, the eigenfunctions and eigenvalues as

$$\psi_i(\eta) = \sin(\mu_i\eta); \quad \mu_i = (2i-1)\pi/2, \quad i = 1,2,3,... \tag{12a,b}$$

It can be shown that the eigenfunctions $\psi_i(\eta)$ present the following orthogonality property:

$$\int_0^1 \psi_i(\eta)\psi_j(\eta)d\eta = \begin{cases} 0, & i \ne j \\ N_i, & i = j \end{cases} \tag{12c,d}$$

where N_i is the normalization integral. Also, we define $\tilde{\psi}_i(\eta)$ as being the normalized eigenfunctions. N_i and $\tilde{\psi}_i(\eta)$ are computed respectively as

$$N_i = \int_0^1 \psi_i^2(\eta)d\eta = 1/2\,; \quad \tilde{\psi}_i(\eta) = \psi_i(\eta)/\sqrt{N_i} \tag{12e,f}$$

Equations (11) and (12) together with the above properties allow the definition of the integral transform pair for the potential $\theta_h(\eta,\xi)$ as:

$$\bar{\theta}_{h,i}(\xi) = \int_0^1 \tilde{\psi}_i(\eta)\theta_h(\eta,\xi)d\eta\,, \qquad \text{transform} \tag{13a}$$

$$\theta_h(\eta,\xi) = \sum_{i=1}^{\infty} \tilde{\psi}_i(\eta)\bar{\theta}_{h,i}(\xi)\,, \qquad \text{inverse} \tag{13b}$$

To obtain the resulting system of differential equations for the transformed potentials $\bar{\theta}_{h,i}(\xi)$, the partial differential equation (10a) is multiplied by $\tilde{\psi}_i(\eta)$, integrated over the domain [0,1] in the η-direction, and the inverse formula, Eq. (13b), is employed in place of the potential $\theta_h(\eta,\xi)$, resulting in the following transformed ordinary differential system:

$$\frac{d^2\bar{\theta}_{h,i}(\xi)}{d\xi^2} + \sum_{j=1}^{\infty} A_{ij}\frac{d\bar{\theta}_{h,j}(\xi)}{d\xi} + \sum_{j=1}^{\infty} B_{ij}\bar{\theta}_{h,j}(\xi) = \bar{g}_i(\xi)\,, \quad i = 1,2,3,... \tag{14a}$$

The same operation can be performed over the initial conditions given by Eqs. (10b,c), to furnish

$$\bar{\theta}_{h,i}(0) = \bar{f}_i\,; \quad \frac{d\bar{\theta}_{h,i}(0)}{d\xi} = 0 \tag{14b,c}$$

where the coefficients in Eqs. (14) are defined as follows:

$$A_{ij} = \frac{1}{\beta}\delta_{ij} + \int_0^1 H(\eta)\tilde{\psi}_i(\eta)\tilde{\psi}_j(\eta)d\eta\,;\; B_{ij} = \frac{1}{\beta}\left[\delta_{ij}\mu_i^2 + \int_0^1 H(\eta)\tilde{\psi}_i(\eta)\tilde{\psi}_j(\eta)d\eta\right];\; \bar{g}_i(\xi) = \bar{g}_{i,1}\cos(\omega\xi) + \bar{g}_{i,2}\sin(\omega\xi) + \bar{g}_{i,3} \tag{15a-c}$$

$$\bar{g}_{i,1} = A\int_0^1 \tilde{\psi}_i(\eta)[\omega^2 - H(\eta)/\beta]d\eta\,;\; \bar{g}_{i,2} = A\omega\int_0^1 \tilde{\psi}_i(\eta)[1/\beta + H(\eta)]d\eta\,;\; \bar{g}_{i,3} = -(1/\beta)\int_0^1 H(\eta)\tilde{\psi}_i(\eta)[1+\theta_e(1+e\eta-e^{\eta})]d\eta \tag{15d-f}$$

$$\bar{f}_i = -\int_0^1 \tilde{\psi}_i(\eta)[1+A+\theta_e(1+e\eta-e^{\eta})]d\eta\,; \quad \delta_{ij} = \begin{cases} 0, & i \neq j \\ 1, & i = j \end{cases} \tag{15g,h}$$

The coefficients may be analytically obtained through symbolic manipulation platforms such as the *Mathematica* system (Wolfram, 1999). Equations (14) form an infinite linear initial value problem, which has to be truncated in a sufficiently high order N, in order to compute the transformed potentials, $\bar{\theta}_{h,i}(\xi)$, to within an user prescribed accuracy target. For the solution of such a system, due to its expected stiff characteristics, specialized subroutines have to be employed, such as the subroutine DIVPAG from the IMSL Library (1991). This subroutine provides the important feature of automatic controlling the relative error over the solution of the ordinary differential equations system, allowing the user to establish error targets for the transformed potentials. Once this system is solved for the transformed potentials, the inverse formula, Eq. (13b), is recalled to provide the potential $\theta_h(\eta,\xi)$, which is added to the filtering potential $\theta_f(\eta;\xi)$, given by Eq. (9e), to furnish the complete temperature field.

In the realm of applications, one might be interested in approximate analytical solutions of the problem here proposed. In order to obtain a fully analytical solution for the system (14), we might recall the so-called lowest order solution of Eqs. (14) (Cotta, 1993), which accounts only for the diagonal terms in the coupling coefficients matrices above. In this way the system becomes decoupled and is rewritten as:

$$\frac{d^2\bar{\theta}_{hl,i}(\xi)}{d\xi^2} + A_{ii}\frac{d\bar{\theta}_{hl,i}(\xi)}{d\xi} + B_{ii}\bar{\theta}_{hl,i}(\xi) = \bar{g}_i(\xi)\,, \quad i = 1,2,3,... \tag{16a}$$

$$\bar{\theta}_{hl,i}(0) = \bar{f}_i\,; \quad \frac{d\bar{\theta}_{hl,i}(0)}{d\xi} = 0 \tag{16b,c}$$

In order to express the analytical solution of system (16), one considers three different situations, namely:

- Case 1: $A_{ii}^2 > 4B_{ii}$:

$$\overline{\theta}_{hl,i}(\xi) = e^{-\frac{A_{ii}}{2}\xi}[C_1 \cosh(\arg \xi) + C_2 \sinh(\arg \xi)] + C_3 \cos(\omega\xi) + C_4 \sin(\omega\xi) + C_5 \tag{17a}$$

$$C_1 = \overline{f}_i - (C_3 + C_5) \tag{17b}$$

$$C_2 = \frac{\frac{A_{ii}}{2}[\overline{f}_i - (C_3 + C_5)] - \omega C_4}{\arg} \tag{17c}$$

- Case 2: $A_{ii}^2 < 4B_{ii}$:

$$\overline{\theta}_{hl,i}(\xi) = e^{-\frac{A_{ii}}{2}\xi}[C_1 \cos(\arg \xi) + C_2 \sin(\arg \xi)] + C_3 \cos(\omega\xi) + C_4 \sin(\omega\xi) + C_5 \tag{18a}$$

$$C_1 = \overline{f}_i - (C_3 + C_5) \tag{18b}$$

$$C_2 = \frac{\frac{A_{ii}}{2}[\overline{f}_i - (C_3 + C_5)] - \omega C_4}{\arg} \tag{18c}$$

- Case 3: $A_{ii}^2 = 4B_{ii}$:

$$\overline{\theta}_{hl,i}(\xi) = e^{-\frac{A_{ii}}{2}\xi}[C_1 + C_2\xi] + C_3 \cos(\omega\xi) + C_4 \sin(\omega\xi) + C_5 \tag{19a}$$

$$C_1 = \overline{f}_i - (C_3 + C_5) \tag{19b}$$

$$C_2 = \frac{A_{ii}}{2}[\overline{f}_i - (C_3 + C_5)] - \omega C_4 \tag{19c}$$

where,

$$\arg = \frac{1}{2}\sqrt{\left|A_{ii}^2 - 4B_{ii}\right|} \tag{20a}$$

$$C_3 = \frac{(B_{ii} - \omega^2)\overline{g}_{i,1} - \omega A_{ii}\overline{g}_{i,2}}{(B_{ii} - \omega^2)^2 + \omega^2 A_{ii}^2} \tag{20b}$$

$$C_4 = \frac{\omega A_{ii}\overline{g}_{i,1} + (B_{ii} - \omega^2)\overline{g}_{i,2}}{(B_{ii} - \omega^2)^2 + \omega^2 A_{ii}^2} \tag{20c}$$

$$C_5 = \frac{\overline{g}_{i,3}}{B_{ii}} \tag{20d}$$

The solutions for each case given by Eqs. (17) to (20) are introduced into the inverse formula (13b), so that the solution for the potential $\theta_h(\eta,\xi)$ is then completed. The potential $\theta_f(\eta;\xi)$, given by Eq. (9e), is then added to the three respective cases above to furnish the approximate analytical temperature field.

3. Results and discussion

Numerical results for the temperature field were obtained from a code developed in the FORTRAN 90/95 programming language. The complete solution was computed using up to five hundred terms ($N \leq 500$) in the eigenfunction expansion, and all the results were obtained with $A = 0.5$, $\theta_e = 0.1$ and taking $H(\eta) = e^{\eta}$, as well as different values of the governing parameters β and ω.

Tables (1) to (4) show the convergence behavior of the temperature distribution along the fin length with different dimensionless relaxation times, and fixed values of dimensionless frequency of base temperature oscillation and dimensionless time. The columns represent the lowest-order solution for the temperature field, with different truncation orders, N, which demonstrate an excellent convergence rate even for N = 50 terms for dimensionless relaxation times $\beta = 0$ and $\beta = 0.1$, as seen in Tables (1) and (2). For higher values of the dimensionless relaxation time, as shown in Tables (3) and (4), the solution yields slower convergence rates evidenced by numerical oscillations, and as a consequence, the complete convergence is reached only with higher truncation orders.

Table 1. Convergence behavior of the temperature field along the fin length for a fixed dimensionless time and $\beta = 0$.

η/N	50	100	200	300	400	500
$\beta = 0, \omega = 1, \xi = 0.5$						
0.45	0.90153	0.90153	0.90153	0.90153	0.90153	0.90153
0.50	0.85589	0.85589	0.85589	0.85589	0.85589	0.85589
0.55	0.81340	0.81340	0.81340	0.81340	0.81340	0.81340
0.60	0.77423	0.77423	0.77423	0.77423	0.77423	0.77423
0.65	0.73858	0.73858	0.73858	0.73858	0.73858	0.73858
0.70	0.70667	0.70667	0.70667	0.70667	0.70667	0.70667
0.75	0.67875	0.67875	0.67875	0.67875	0.67875	0.67875
0.80	0.65511	0.65511	0.65511	0.65511	0.65511	0.65511
0.85	0.63605	0.63605	0.63605	0.63605	0.63605	0.63605
0.90	0.62194	0.62194	0.62194	0.62194	0.62194	0.62194

Table 2. Convergence behavior of the temperature field along the fin length for a fixed dimensionless time and $\beta = 0.1$.

η/N	50	100	200	300	400	500
$\beta = 0.1, \omega = 1, \xi = 0.5$						
0.45	0.91154	0.91401	0.91032	0.91186	0.91128	0.91129
0.50	0.86540	0.86656	0.86720	0.86745	0.86759	0.86768
0.55	0.82715	0.82777	0.82677	0.82718	0.82703	0.82702
0.60	0.79093	0.78923	0.78956	0.78969	0.78976	0.78981
0.65	0.75591	0.75642	0.75578	0.75604	0.75594	0.75594
0.70	0.72491	0.72536	0.72560	0.72569	0.72574	0.72578
0.75	0.69941	0.69974	0.69923	0.69944	0.69936	0.69936
0.80	0.67777	0.67671	0.67692	0.67700	0.67704	0.67707
0.85	0.65906	0.65940	0.65894	0.65913	0.65906	0.65906
0.90	0.64509	0.64544	0.64562	0.64570	0.64574	0.64576

Table 3. Convergence behavior of the temperature field along the fin length for a fixed dimensionless time and $\beta = 1$.

η/N	50	100	200	300	400	500
$\beta = 1, \omega = 1, \xi = 0.5$						
0.45	0.85316	0.87114	0.84997	0.86179	0.85351	0.85990
0.50	0.42152	0.41924	0.41810	0.41772	0.41753	0.41741
0.55	0.03323	0.01332	0.03815	0.02430	0.03400	0.02652
0.60	0.00451	0.03127	0.02680	0.02531	0.02457	0.02412
0.65	0.01418	0.00811	0.01775	0.01239	0.01614	0.01325
0.70	0.01710	0.01192	0.00933	0.00847	0.00803	0.00777
0.75	0	0	0	0	0	0
0.80	0	0	0	0	0	0
0.85	0	0	0	0	0	0
0.90	0	0	0	0	0	0

Table4. Convergence behavior of the temperature field along the fin length for a fixed dimensionless time and $\beta = 5$.

η/N	50	100	200	300	400	500
$\beta = 5.0, \omega = 1, \xi = 0.5$						
0.15	1.09470	1.11360	1.11190	1.10550	1.10930	1.11040
0.20	1.06010	0.97408	1.00490	1.00630	0.99611	0.98812
0.25	-0.03309	-0.00131	-0.00178	0.02307	0.00957	0.00476
0.30	0.03372	0.01623	0.00584	0.00589	0.00989	0.01286
0.35	0.01637	0.00600	0.00686	0.01290	0.00947	0.00835
0.40	-0.00292	0.01214	0.00681	0.00681	0.00880	0.01029
0.45	0.00536	0.00572	0.00633	0.01015	0.00797	0.00726
0.50	0.01590	0.00940	0.00556	0.00555	0.00698	0.00805
0.55	0.00766	0.00410	0.00458	0.00753	0.00585	0.00530
0.60	-0.00235	0.00654	0.00341	0.00340	0.00456	0.00543

Figure (2) analyzes the influence of the dimensionless relaxation time on the temperature field along the fin length. Also in this figure is offered a comparison with the results of Lin (1998). The governing parameters utilized were $\omega = 1.0$, $\xi = 0.5$ and $\beta = 0$, 0.1, 1 and 5. As can be seen from this figure, for lower values of dimensionless relaxation time, the thermal wave propagates very fast, as a result of the speed of propagation approaching infinity, on the other hand, for higher values of β, the thermal wave does not reach the fin tip, and extinguishes at approximately $\eta = 0.55$ for $\beta = 1.0$, and at $\eta = 0.24$ for $\beta = 5.0$. This figure also illustrates the good agreement between the present results with those of Lin (1998).

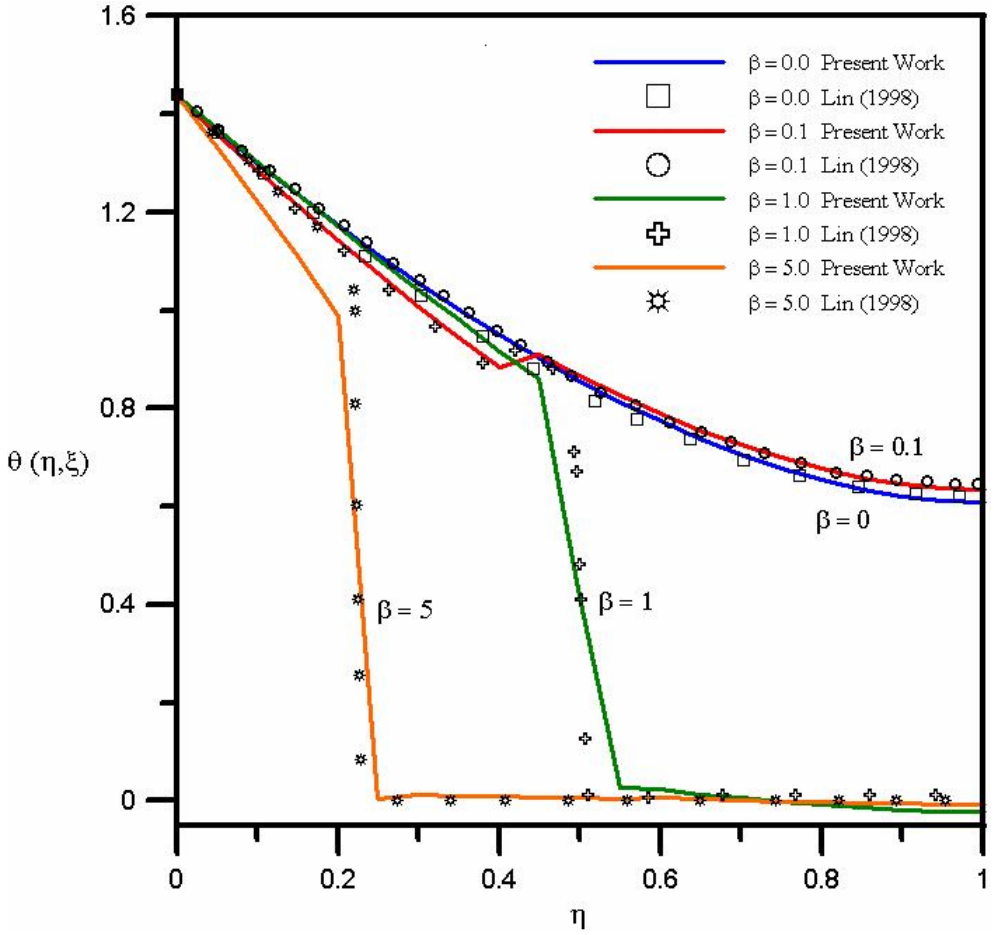

Figure 2. Temperature distribution along the fin length for different dimensionless relaxation times: $\omega = 1.0$ and $\xi = 0.5$.

Figure (3) shows the temperature distribution along the fin length with different dimensionless frequencies of base temperature oscillation, ω. Once again, it is offered a comparison of the present results with those of Lin (1998), which shows a good agreement. This figure makes it evident that even increasing the parameter ω, the thermal wave remains extinguished at $\eta = 0.55$ for $\beta = 1.0$, i.e., the dimensionless frequency of base temperature oscillation does not affect the extent of the non-Fourier effect along the fin length. The good agreement between the present results with those of Lin (1998) demonstrates that the lowest-order solution can give reasonable estimates of the hyperbolic conduction effects caused by the non-Fourier model, offering a straightforward analytical solution representation of this complex formulation.

Figure (4) investigates the effect of the dimensionless relaxation time on the temperature field at the fin tip while varying the dimensionless time. This figure demonstrates that for lower values of β, the fin tip temperature rapidly increases, as expected, because these values of β agree with the classical Fourier model, in which the thermal waves are propagated with a infinite speed. For higher values of dimensionless relaxation time, the fin tip is not immediately excited by the application of the thermal pulse. It is observed that the temperature gradually increases after a short time period, and the phase shift that appears among the curves is influenced by the dimensionless relaxation time, once the heat flow does not begin right afterwards, there is an interval of time between the application of the temperature gradient and the heat flow, which is exactly the period of storage of energy. Also, the comparison with the results of Lin (1998) again reconfirms the good agreement, although one may observe deviations, especially for higher values of β. However, for most practical purposes, the lowest-order solution can be employed as a good approximation of the hyperbolic heat conduction behavior.

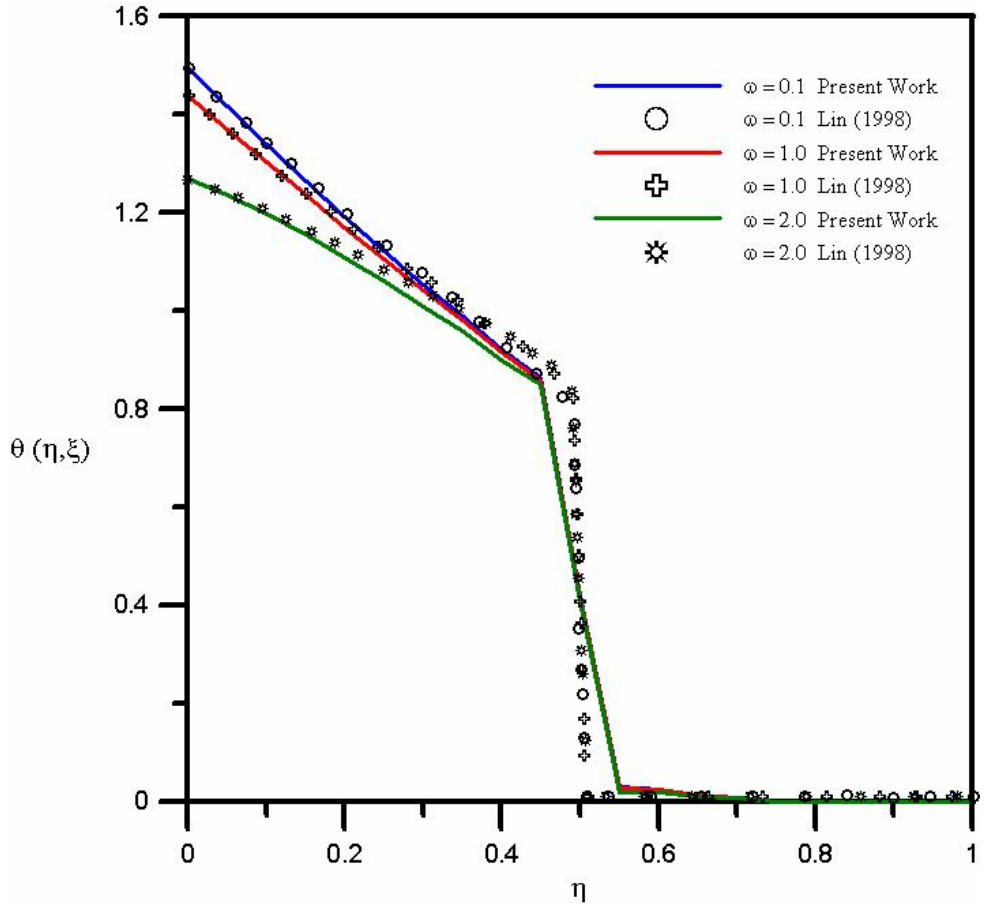

Figure 3. Temperature distribution along the fin length for different dimensionless frequencies of base temperature oscillation: $\beta = 1.0$ and $\xi = 0.5$.

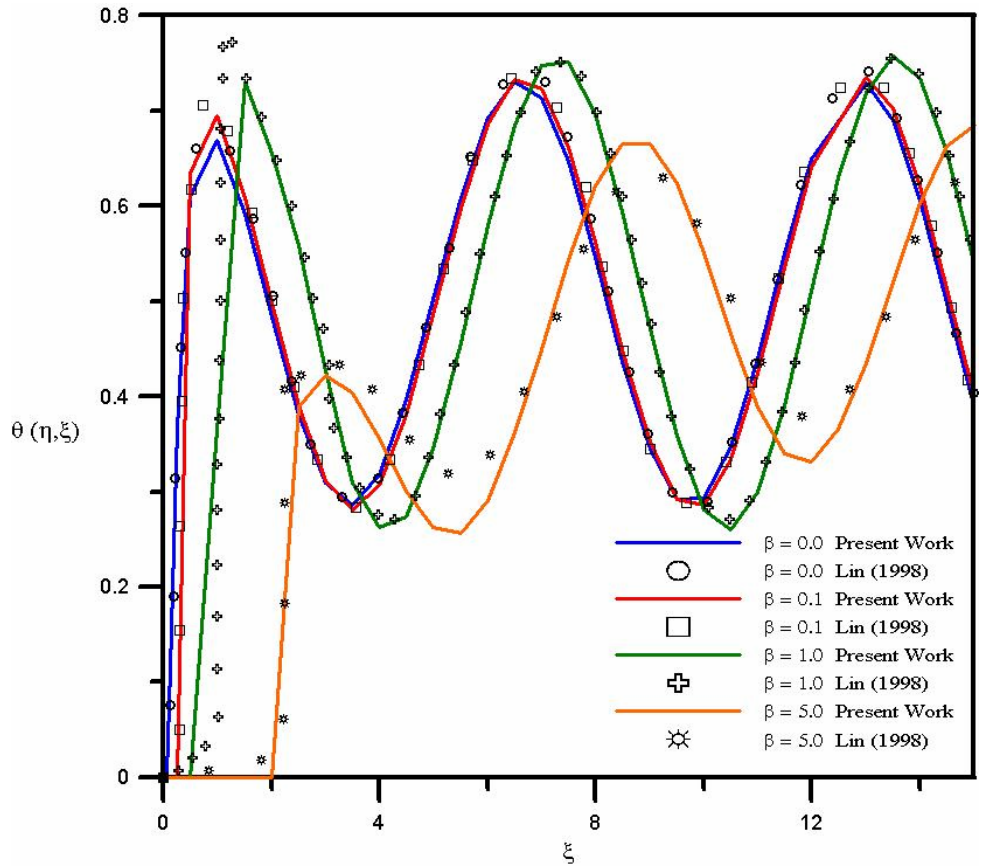

Figure 4. Temperature evolution at the fin tip for different dimensionless relaxation times ($\omega = 1.0$).

4. Conclusions

Hyperbolic heat conduction for a convective fin of constant cross-section area, submitted to periodic thermal conditions, has been analyzed using the Generalized Integral Transform Technique (GITT). A lowest-order solution was obtained in analytic form, offering approximate results for the fin temperature distribution for the investigated ranges of the governing parameters. It could be verified that the non-Fourier effect is significant for short times in the rectangular fin analysis, during the initial transient, when the thermal wave fronts are observed.

5. Acknowledgments

The authors would like to acknowledge the financial support provided by CNPq and FAPERJ.

6. References

Cattaneo, C., 1958, “Sur une Forme de L'équation de la Chaleur Eliminant le Paradoxe d´une Propagation Instantanée”, Comptes Rendus Hebdomadaires des Seances de L’Academie des Sciences, Vol. 24*7*, pp. 431-433.

Cotta, R.M., 1993, “Integral Transforms in Computational Heat and Fluid Flow”, CRC Press, Boca Raton, USA.

Cotta, R. M., 1994, “Benchmark Results in Computational Heat and Fluid Flow: - The Integral Transform Method”, Int. J. Heat Mass Transfer (Invited Paper), Vol. 37 (Suppl. 1), pp. 381-393.

Cotta, R.M. and Mikhailov, M.D., 1997, “Heat Conduction: Lumped Analysis, Integral Transforms, Symbolic Computation”, Wiley-Interscience, USA.

Cotta, R.M., and Mikhailov, M.D., 2006, “Hybrid Methods and Symbolic Computations”, in: Handbook of Numerical Heat Transfer, 2nd edition, Chapter 16, Eds. W.J. Minkowycz, E.M. Sparrow, and J.Y. Murthy, John Wiley, New York, pp.493-522.

Cruz, A.G.B., Macêdo, E.N. and Quaresma, J.N.N., 2001, One-dimensional Hyperbolic Heat Conduction Analysis through Finite Volume and Gear Methods, Proceedings of 16th Brazilian Congress of Mechanical Engineering, Uberlândia, Brazil, Paper code TRB0071.

IMSL Library, 1991, Math/Lib, Houston, Texas.

Lin, J. Y, 1998, “The non-Fourier Effect on the Fin Performance under Periodic Thermal Conditions”, Applied Mathematical Modelling, Vol. 22, pp. 629-640.

Macêdo, E.N., Monteiro, E.R. and Quaresma, J.N.N., 2005, “One-Dimensional Hyperbolic Heat Conduction Analysis through Integral Transform Method”, Proceedings of the 4th International Conference on Computational Heat and Mass Transfer**,** Paris-Cachan, France.

Quaresma, J.N.N., Macêdo, E.N. and Cruz, A.G.B., 2001, “Hybrid Solution in Hyperbolic Heat Conduction: Laplace Transform with Numerical Inversion”, Proceedings of the 2nd International Conference on Computational Heat and Mass Transfer, Rio de Janeiro, Brazil.

Tsai, C.S., Lin, Y.C. and Hung, C.I., 2005, “A Study on the non-Fourier Effects in Spherical Media due to Sudden Temperature Changes on the Surfaces”, Heat and Mass Transfer, Vol.41, pp. 706-716.

Vernotte, P., 1958, “Les Paradoxes de la Theorie Continue de L'Équation de la Chaleur”, Comptes Rendus Hebdomadaires des Seances de L’Academie des Sciences, Vol. 246, pp. 3154-3155.

Wolfram, S., 2003, “The *Mathematica* Book”, 5th ed., Wolfram Media.

7. Copyright Notice